Carcinogenesis vol.33 no.2 pp.436–441, 2012
doi:10.1093/carcin/bgr260
Advance Access publication November 18, 2011

Epigenetic subclassification of meningiomas based on genome-wide DNA methylation analyses

Yugo Kishida[1], Atsushi Natsume[1,*], Yutaka Kondo[2], Ichiro Takeuchi[3], Byonggu An[2], Yasuyuki Okamoto[2], Keiko Shinjo[2,4], Kiyoshi Saito[5], Hitoshi Ando[1,5], Fumiharu Ohka[1], Yoshitaka Sekido[2,4] and Toshihiko Wakabayashi[1]

[1]Department of Neurosurgery, Nagoya University School of Medicine, 65 Tsurumai-cho, Showa-ku, Nagoya, Aichi 466-8550, Japan, [2]Division of Molecular Oncology, Aichi Cancer Center Research Institute, 1-1 Kanokoden, Chikusa-Ku, Nagoya, Aichi 464-8681, Japan, [3]Department of Scientific and Engineering Simulation, Graduate School of Engineering, Nagoya Institute of Technology, Nagoya, Aichi 466-8555, Japan, [4]Department of Cancer Genetics, Nagoya University Graduate School of Medicine, 65 Tsurumai-cho, Showa-ku, Nagoya, Aichi 466-8550, Japan and [5]Department of Neurosurgery, Fukushima Medical University, 1 Hikarigaoka, Fukushima 960-1295, Japan

[*]To whom correspondence should be addressed. Tel: +81 52 744 2353; Fax: +81 52 744 2360;
Email: anatsume@med.nagoya-u.ac.jp

Meningiomas are among the most common intracranial tumors and are mostly curable by surgical resection. However, some populations of meningiomas with benign histological profiles show malignant behavior. The reasons for this inconsistency are yet to be ascertained, and novel diagnostic criteria other than the histological one are urgently needed. The aim of the present study is to subclassify meningiomas from the viewpoint of gene methylation and to determine the subgroup with malignant characteristics. Thirty meningiomas were analyzed using microarrays for 6157 genes and were classified into three clusters on the basis of their methylation status; these were found to be independent of the histological grading. One of the clusters showed a high frequency of recurrence, with a marked accumulation of methylation in a subset of genes. We hypothesized that the aggressive meningiomas universally share characteristic methylation in certain genes; therefore, we chose the genes that strongly contributed to cluster formation. The quantified methylation values of five chosen genes (*HOXA6*, *HOXA9*, *PENK*, *UPK3A* and *IGF2BP1*) agreed well with microarray findings, and a scoring system consisting of the five genes significantly correlated with a high frequency of recurrence in an additional validation set of 32 patients. Of particular note is that three cases with malignant transformation already showed hypermethylation at histologically benign stage. In conclusion, a subgroup of meningiomas is characterized by aberrant hypermethylation of the subset of genes in the early stage of tumorigenesis, and our findings highlight the possibility of speculating potential malignancy of meningiomas by assessing methylation status.

Introduction

Meningiomas account for 24–30% of primary intracranial tumors with clinical malignancy, principally predicted by histological grading based on World Health Organization (WHO) criteria. Grade I meningiomas are considered benign and curable by appropriate surgical resection, grade II (intermediate grade/atypical) meningiomas have a high recurrence rate reaching 40% per 5-year period and grade III (anaplastic) show the worst prognosis (1–3). However, some grade I meningiomas show early or frequent recurrence similar to higher-grade meningiomas, despite their benign histological profile. To resolve this discrepancy, in 2007, the WHO revised their criteria based on morphological findings, emphasizing on mitotic activity and brain invasion (4,5); however, so far, there has been no interobserver and interinstitutional uniformity in the pathological diagnosis. One of the reasons for this inconsistency is the histological similarities between tumors in each grade, as high-grade meningiomas are generally considered to progress from lower-grade meningiomas (6). Furthermore, in some grade I meningiomas, recurrent tumors clearly display a histologically benign profile with no discernable difference from non-recurrent types. The Simpson grade is a clinical grading scale used to classify the extent of postoperative residual tumor, and it has been used as a predictor for recurrence. However, the Simpson grade is highly subjective, with its predictive outcome varying among surgeons. These facts indicate the limitations of using a histological and surgical classification system to grade tumors. There is, thus, an urgent need for a non-histological subclassification or marker system that reflects potential malignant characteristics of meningiomas.

The biological marker *S100A5* (7), the loss of *NDRG2* (8) and the suppression of *NF2* homologs and interacting proteins such as *DAL-1* and *TSLC1* (9,10) have been linked with the aggressiveness of meningiomas. In recent years, epigenetic alterations represented by gene methylation have drawn attention as one of the most compelling research subjects. The reasons for this are that various epigenetic alterations occur in the early stages of tumorigenesis (11) and are potentially reversible by epigenetic-regulating agents. However, biomarkers to predict the potential aggressiveness of histologically benign meningiomas have not been conclusively established; only the promoter hypermethylation of *TIMP3* has been reported as a marker of malignancy in grade III meningiomas (12). However, since gene methylation occurs as a result of diverse alterations in widespread loci of the genome in various subtypes of tumors, comprehensive genome-wide DNA methylation analysis is warranted.

In the present study, we subclassified histologically benign and intermediate-grade meningiomas into three subgroups based on a genome-wide methylation analysis. The subclassifications were found to correlate well with clinical recurrence/progression but not with classical predictors, e.g. histological grades, Simpson grades and age. Furthermore, we selected five hub genes from hypermethylated genes in the clinical malignant cluster and established a scoring system. The simplified scoring system showed high reproducibility in the validation samples. Our findings indicated the presence of subgroups with potential malignant characteristics in conjunction with methylation status and the possibility of prediction by the methylation quantification in several genes.

Abbreviations: CIMP, CpG island methylator phenotype; MCAM, methylated CpG island amplification microarray; WHO, World Health Organization.

Materials and methods

Collection of tumor and control tissues

Forty-three samples of frozen meningioma tissue (WHO grades I and II) were retrospectively randomly selected. After DNA quality check, 20 samples of WHO grade I and 10 of WHO grade II meningiomas were finally chosen. The clinical information of the patients is shown in accordance with reporting recommendation for tumor marker prognostic studies criteria (13) in Supplementary Table 1 (available at *Carcinogenesis* online; 17 females and 13 males; mean age 56.3 years, range 30–80 years). The mean follow-up period was 48 months (11–100 months) after surgery, and 10 cases had a relapse during the follow-up period. All patients had been operated on at Nagoya University Hospital, Nagoya, Japan, by a regular surgeon and two assistants.

Normal control dura mater samples of both genders were obtained from autopsy sourced from Nagoya University. DNA methylation microarray requires gender-matched controls because of the influence of X chromosome imprinting in females. All patients provided written informed consent for using excised specimens for genetic research.

In addition, we randomly collected 32 formalin-fixed paraffin-embedded samples from our affiliated hospitals as a validation set (Supplementary Table 2, available at *Carcinogenesis* online). The validation set consisted of

13 tumors classified as WHO grade I and 19 tumors classified as WHO grade II. There was no bias between the two sample sets in terms of clinical features, such as age, Simpson grade, gender and postoperative treatments.

Tumor recurrence/progression was evaluated by magnetic resonance imaging at the 3-month intervals on the basis of Response Evaluation Criteria In Solid Tumors guideline version 1.1.

Genomic DNA extraction and bisulfite treatment

Genomic DNA was isolated from 20–25 mg of fresh-frozen samples or five slices (10 μm per slice) of formalin-fixed paraffin-embedded samples using QIAamp DNA Mini Kit (QIAGEN, Tokyo, Japan). Deparaffinization using xylene and ethanol was carried out for formalin-fixed paraffin-embedded samples before DNA extraction. Extracted DNA (1 μg) was then subjected to bisulfite conversion using EpiTect Bisulfite Kit (QIAGEN) and diluted to 10 ng/μl before polymerase chain reaction amplification.

Methylated CpG island amplification microarrays

Global analysis by methylated CpG island amplification microarrays (MCAMs) using genomic DNA from meningiomas and control specimens was carried out.

MCAM was performed according to methods described previously (14). Briefly, 2 μg of genomic DNA was digested with 100 U methylation-sensitive restriction endonuclease SmaI (New England Biolabs, Ipswich, MA) for 8 h at 20°C. This step was repeated. Subsequently, the DNA was digested with 20 U methylation-insensitive restriction endonuclease XmaI for 9 h at 37°C. Digested DNA (500 ng) was ligated to adaptors. After filling in the overhanging ends of the ligated DNA fragments at 72°C, DNA was amplified using 100 pmol of RMCA24 primer under the following reaction conditions: 95°C for 3 min, 25 cycles of 1 min at 95°C and 3 min at 77°C. The products were labeled with Cy5 (red) for tumor samples and Cy3 (green) for control samples using a random-primed Klenow polymerase reaction (Invitrogen, Carlsbad, CA) at 37°C for 3 h. The labeled samples were then hybridized to the custom-made 4 × 44K human promoter array containing 15 134 probes corresponding to 6157 unique genes (Agilent, Santa Clara, CA) in the presence of human Cot-1 DNA for 40 h at 65°C. After the arrays were washed according to the manufacturer's protocol, they were scanned on an Agilent scanner using Feature Extraction software (Agilent).

Quantification of promoter methylation by bisulfite pyrosequencing

To validate the results of MCAMs, we quantified methylation rate by bisulfite pyrosequencing. Primers for bisulfite pyrosequencing were designed by PSQ assay design (Biotage AB, Kungsgatan, Sweden). For all genes, the reproducibility and quantitative capability were confirmed using SssI methylase-treated DNA (New England Biolabs) as a positive control, peripheral blood DNA as a negative control, both these types of DNA mixed in equal quantities and sample DNA. The primer sequences are listed in Supplementary Table 3 (available at *Carcinogenesis* online). The bisulfite pyrosequencing was carried out according to methods described previously (15,16). The methylation rates at different CpG sites measured by pyrosequencing were averaged to represent the methylation levels of these genes. The conditions for polymerase chain reaction products were confirmed by electrophoresis with 3% agarose gel. In our previous articles, genes with methylation levels >15% were considered methylation positive because lower values could not easily be distinguished from background (17,18).

Analyses of MCAMs and statistical tools

The ratio of tumor signal to control signal calculated from the MCAM results was described as the signal ratio. To avoid an artificial effect of excess value, signal ratios >10 and control signals <600 were corrected to 10 and 600, respectively. A signal ratio with ≥2 increment was considered hypermethylation on the basis of our previous study (16), and the reliability of this criterion in the present study was confirmed using bisulfite pyrosequencing technique. The hierarchical cluster analysis for 6157 genes was performed using Cluster 3.0 software based on an agglomerative hierarchical clustering algorithm (http://rana.lbl.gov/EisenSoftware.htm), and the heat map was constructed using Java TreeView.

Consensus clustering has recently been used in many biomedical studies (19) because it can provide statistical stabilities of the identified clusters. Within the consensus clustering, *k*-means clustering with the Euclidean distance metric was used as the basic clustering option. For *k* ranging from 2 to 5, the *k*-means clustering was run >10 000 iterations with the subsampling ratio of 0.8 for estimating the consensus matrix. For the purpose of visualization and cluster identification, hierarchical clustering with the Euclidean distance metric and the complete linkage option was applied to the estimated consensus matrix. The identified clusters were validated and confirmed using consensus cluster dependence factor plot analysis (20). The analysis of variance between clinical features and clusters was performed by the Kruskal–Wallis test using PASW Statistic (SPSS, Chicago, IL), and the Games–Howell test was added if a feature was significantly different among clusters. The significance of *P* value in each test was determined at $P < 0.05$.

To identify the genes showing significant differences among clusters, we calculated the *P* value by the Kruskal–Wallis test using the statistical software R (R foundation, Vienna, Austria), and we chose genes satisfying $P < 0.01$. To avoid false positives with genes with low signal ratios, the genes commonly methylated in more than one-third of any three clusters were selected according to our previous study (17). In addition, the pathway analysis using GeneSpring GX (Agilent) was performed for further refinement of genes.

Results

Quality assurance of MCAMs

MCAMs were performed by a two-color method matched to the same-gender control samples, and the reliability of MCAMs and the criteria for it were assured before data analyses. The dye swap experiment using the same sample (case #3) showed good reproducibility with a high determination coefficient ($R^2 = 0.819$; Figure 1A). Subsequently, to validate our criterion for hypermethylation (≥2 increment of the signal ratio) in this study, a signal ratio of five arbitrarily selected genes (*REC8*, *CHAD*, *HIF3A*, *UPK3A* and *SPOCK2)* in MCAMs was compared with the quantitative methylation values of the genes in bisulfite pyrosequencing. The quantitative capability and reproducibility of bisulfite pyrosequencing in these five genes had been previously confirmed using SssI methylase-treated DNA, peripheral blood DNA and tumor samples (data not shown). The positive test of methylation in bisulfite pyrosequencing was defined as 15% in accordance with previous studies (17,18,21,22) because lower values could not easily be distinguished from background. In addition, the methylation level of the five genes in normal dura matter was 13–15% (data not shown). As shown in Figure 1B, our criterion based on signal ratio correlated well with the actual quantitative values and showed acceptable sensitivity and specificity (89 and 86%, respectively).

MCAMs classification correlates with recurrence in meningiomas

Thirty meningiomas were distributed bimodally according to the number of methylated genes (Figure 1C). The unsupervised hierarchical cluster analysis classified 30 meningiomas into three clusters (clusters 1–3) based on the similarity of the methylation pattern (Figure 1D). The mean number of hypermethylated genes (signal ratio ≥2) in samples classified into clusters 1–3 was 164.6, 323.4 and 345.6, respectively (cluster 1 versus clusters 2 and 3; $P < 0.001$). The heat map in Figure 1D displays the 198 significantly different genes among the clusters. Eight of nine samples with >350 hypermethylated genes shown in Figure 1C were clustered into cluster 1, whereas less methylated tumors with <200 methylated genes completely were classified into cluster 1. Due to the limited sample size, we conducted consensus clustering analysis in which *k*-means clustering was used as the base clustering method and the number of clusters $k = 2$–5 were examined. Supplementary Figure 1A, available at *Carcinogenesis* online, displays the dendrograms and heat maps of the consensus matrix for $k = 2$–5. The figure indicates that the clustering stability increases for $k = 2$ and 3 but not for $k = 4$ and 5 (Supplementary Figure 1B, available at *Carcinogenesis* online). We examined the members of the three clusters identified in the consensus matrix (for $k = 3$) and found that they almost perfectly match with the original three clusters in Figure 1D (Supplementary Figure 1C, available at *Carcinogenesis* online).

Clinical features, including gender, age, WHO grade, Simpson grade, perifocal edema and recurrence, were statistically compared between the three clusters. The proportion of the WHO grades did not show a significant correlation with cluster formation ($P = 0.417$). Similarly, age, Simpson grade and perifocal edema did not correlate with the subclassification based on methylation status ($P = 0.891$, 0.863 and 0.374, respectively). In contrast, male and recurrence were significantly different among clusters ($P = 0.001$ and 0.004, respectively). Compared with cluster 1, male cases were significantly

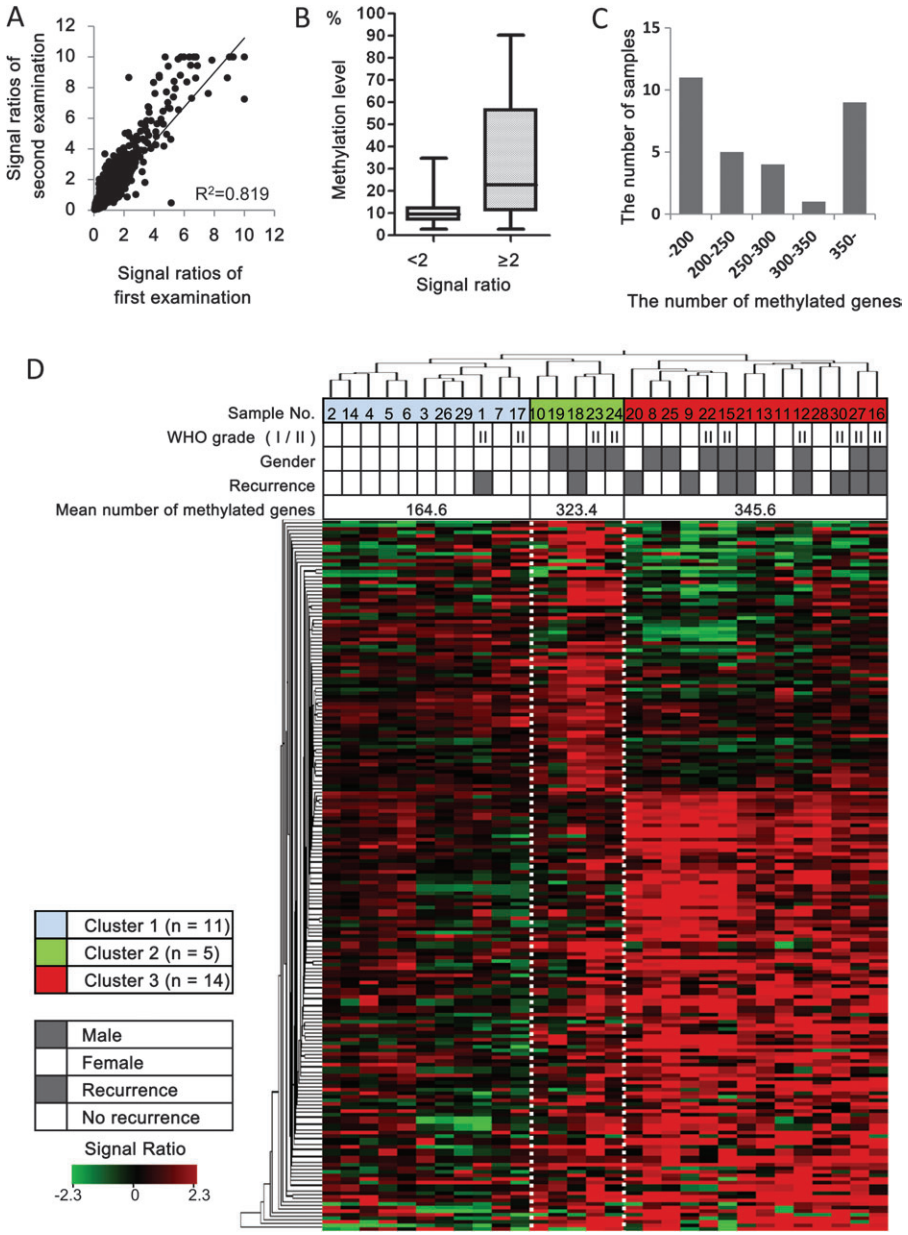

Fig. 1. MCAM analyses in meningiomas. (**A**) Confirmation of the reproducibility of MCAMs. The dots represent signal ratios in dye swap experiment. The results obtained by two microarrays showed high reproducibility despite differences caused by the binding efficiency of the two dyes. (**B**) Validation for the criterion of methylation in MCAMs. A signal ratio of >2 corresponds well with high-quantified values in bisulfite pyrosequencing in five genes (*REC8*, *CHAD*, *HIF3A*, *UPK3A* and *SPOCK2*) in 111 experiments. The positive test for methylation in bisulfite pyrosequencing was defined as ≥15% on the basis of previous studies (see Materials and methods). The sensitivity and specificity of MCAMs for methylation were, respectively, 89 and 86%. (**C**) Bimodal distribution of tumor samples according to the number of methylated genes. A genome-wide methylation analysis (MCAM) showed that samples were distributed into low-/high-methylation groups. (**D**) Dendrogram and heat map overview of the unsupervised hierarchical clustering analysis. Thirty meningiomas were classified into three clusters (clusters 1–3) based on the methylation status in 6157 genes. Clusters 2 and 3 included significantly large number of males compared with cluster 1 ($P = 0.035$ and 0.001, respectively). The recurrent cases tended to accumulate in cluster 3 compared with clusters 1 and 2 ($P = 0.004$ and 0.081, respectively). The heat map based on 198 genes (Supplementary Table 4, available at *Carcinogenesis* online) showed characteristic accumulation of methylation in clusters 2 and 3, despite cluster 1 being defined as the low methylator phenotype.

involved in clusters 2 and 3 ($P = 0.035$ and 0.001, respectively), and more interestingly, recurrent cases accumulated in cluster 3 as compared with clusters 1 and 2 ($P = 0.004$ and 0.081, respectively).

A novel scoring system associated with meningioma recurrence/progression

The list of 198 genes in total, with significant differences among clusters ($P < 0.01$) and accumulation of methylated samples in any of the clusters, is shown in Supplementary Table 4 (available at *Carcinogenesis* online). From these genes, to estimate the correlation with recurrence, 113 genes that were frequently methylated in cluster 3 were chosen and were applied to the pathway analysis. We selected seven hub genes, which regulate other genes (Supplementary Figure 2, available at *Carcinogenesis* online, black squares). The chosen genes were quantified by bisulfite pyrosequencing, and the genes with unstable polymerase chain reaction amplification before pyrosequencing were excluded. Finally, five genes (*HOXA6*, *HOXA9*, *PENK*, *UPK3A* and *IGF2BP1*) were retained.

The quantitative values of the five genes corresponded well with the results of MCAMs among clusters (Figure 2A). Here, we established

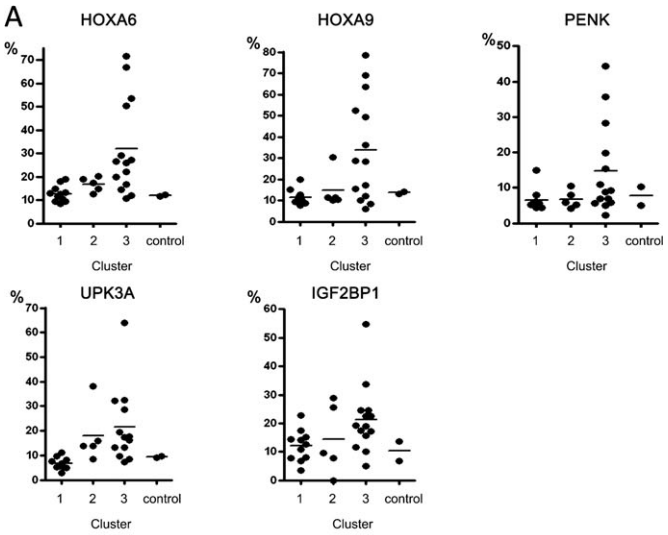

B

Gene / Methylation	HOXA6	HOXA9	PENK	UPK3A	IGF2BP1
≥30 %	3	3	3	3	3
≥15 %	2	2	2	2	2
<15 %	1	1	1	1	1

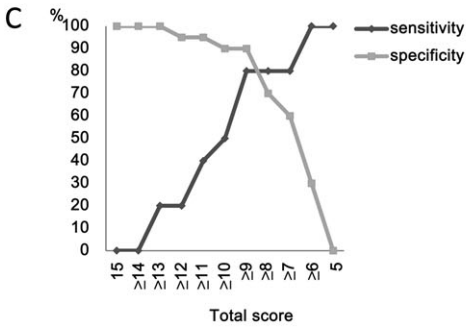

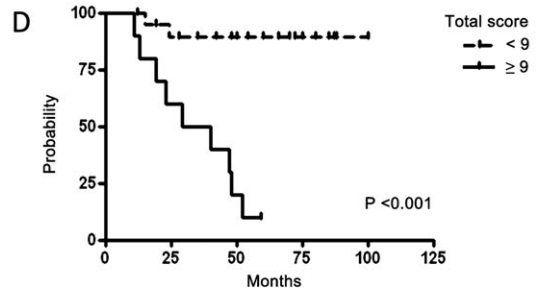

Fig. 2. Scoring system based on MCAMs for the speculation of recurrence. (**A**) The correlation between the methylation status of five chosen genes (*HOXA6*, *HOXA9*, *PENK*, *UPK3A* and *IGF2BP1*) and the results of clustering analysis was validated. The dots represent the methylation level by bisulfite pyrosequencing, and the black lines in the graph represent averages in each cluster. (**B**) A novel scoring system based on methylation level of five genes. Each gene was given points from 1 to 3, with a total score of 5–15, according to quantified values in bisulfite pyrosequencing. (**C**) Determination of cut-off in the scoring system for prediction of recurrence in 30 meningiomas. A total score of ≥9 was adopted according to both high sensitivity and specificity (80 and 90%, respectively). (**D**) Progression-free survival curve based on cut-off scores of ≥9 in 30 meningiomas.

a scoring system on a scale of 5–15 points, comprising three stages depending on the methylation values of the five genes (Figure 2B). Score 1 category was defined as <15%, corresponding to the negative test of methylation. On the other hand, hypermethylation of 30% and more was categorized into score 3 because certain patients showed marked hypermethylation, indicating another phenotype (Figure 2A).

On the basis of this scoring system, a total score of >9 points showed the highest sensitivity and specificity for recurrence in 30 patients analyzed by MCAMs (Figure 2C; 80 and 90%, respectively). The progression-free survival curve of 30 patients divided by scores of 9 and above is shown in Figure 2D.

To validate the universal applicability of this scoring system in meningiomas, the system was applied to 32 additional meningiomas collected from other hospitals. As was found in the initially analyzed 30 cases, five genes demonstrated apparent hypermethylation in the recurrent group, although only *UPK3A* did not show any statistical significance (Figure 3A). The progression-free survival curve divided at point 9 or above in our scoring system showed significant differences in the validation samples as well (Figure 3B). It is imperative to perform a multivariate analysis to show that the methylation index is independent of other clinical variables such as grade, age and gender. We have combined the test and validation samples (62 cases in total) for multivariate analysis. As shown in Figure 3C, tumor progression was significantly correlated with scores ≥9 but not with age, WHO grade, gender or Simpson grade.

Interestingly, three patients experienced malignant transformations at the recurrence, and the characteristics of their hypermethylation patterns were already observed at the first surgery when they were diagnosed with grade I meningiomas (Figure 3D).

Discussion

For meningiomas, most of the previous studies on methylation markers have targeted mainly a few known genes associated with cell proliferation, mitogenesis or oncogenesis, such as maternally expressed gene 3 (*MEG3*) (23), *RASSF1A* (24), *uPA* (25) and the tissue inhibitor of metalloproteinase 3 (*TIMP3*) (12). *TIMP3* methylation is the generally acknowledged epigenetic marker of meningioma progression; however, it chiefly occurs in grade III (anaplastic) meningiomas and to a lesser extent in grade I and II meningiomas (17 and 22%, respectively). Therefore, a crucial methylation marker to predict an aggressive subtype in the early stage of meningiomas remains to be established, despite a need for it. Moreover, the studies targeting single key genes always confront the problem of whether such genes are actually responsible for the formation of tumor characteristics per se or are a part of extensive alterations associated with carcinogenesis. These problems prompted us to consider the necessity of genome-wide analyses for methylation status to comprehend tumor characteristics. Here, we investigated the global methylation status of low-grade meningiomas with the aim of reclassification and compensation of the histological classification. MCAMs revealed the presence of three clusters in grade I and II meningiomas. Cluster 1 showed clinically benign courses, whereas cluster 3 was characterized by a high frequency of recurrence and/or progression and accumulated hypermethylation in this subset of genes. On the other hand, although cluster 2 showed interesting aspects of methylation, it did not correlate with any of the patients' clinical features, except with gender, because of the low number of patients in this cluster. This cluster might be a completely different subgroup from the other two clusters. Further studies using a larger number of patient samples are needed to understand the implications of this subgroup. In addition, there are substantial differences in normal epigenetic patterns between genders. To exclude the possibility that the defining features of one cluster compared with another could be an artifact of gender biases, we have performed multivariate analysis in each gender separately in combined test and validation sample sets (62 cases in total). As shown in Supplementary Figure 3A (available at *Carcinogenesis* online), the effect with recurrence still held up even when separated into male and female groups. Moreover, patients with low scores (<9 points) experienced significantly longer progression-free survival in both genders (Supplementary Figure 3B, available at *Carcinogenesis* online).

Noushmehr *et al.* reported the presence of CpG island methylator phenotype (CIMP), a characteristic accumulation of promoter methylation

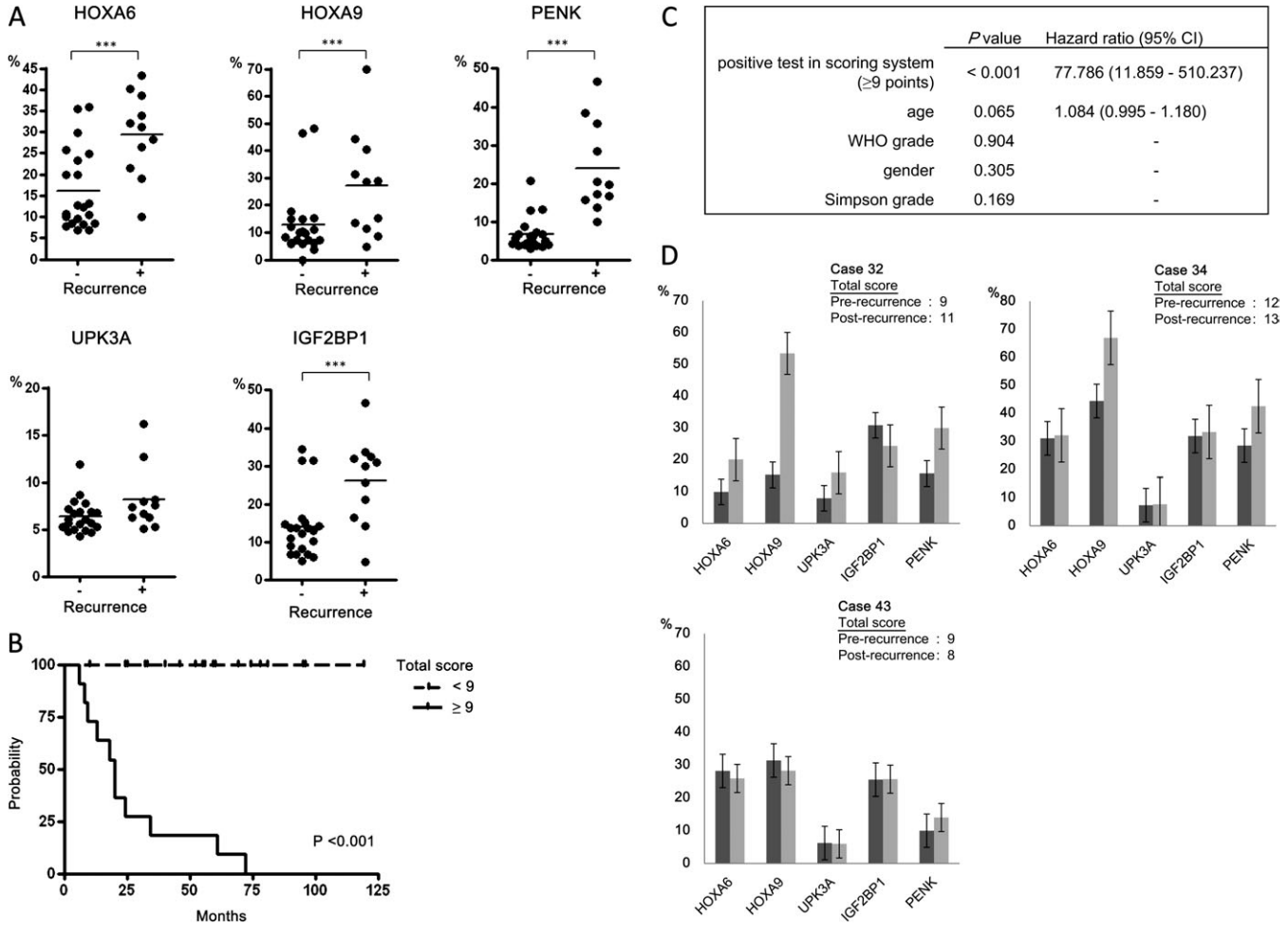

Fig. 3. Validation of the scoring system in another sample set. (**A**) Methylation status of five genes in validation set from another 32 patients. The promoter methylation accumulated in recurrent cases as frequently as 30 patients analyzed by MCAMs. $^{***}P < 0.001$. (**B**) Progression-free survival curve for the validation set. The hypermethylated samples with ≥9 in the scoring system demonstrated marked correlation with recurrence. (**C**) We have combined the test and validation samples (62 cases in total) for multivariate analysis. Tumor progression was significantly correlated with scores ≥9 but not with age, WHO grade, gender or Simpson grade. (**D**) The total scores in the three cases that were recurrent with malignant transformation. The high methylator phenotypes were observed before recurrence.

into a subset of genes in the particular subtype of the tumors, in human glioblastomas and the possibility of detailed subclassification for the prediction of a good prognostic subgroup based on CIMP presence (26–28). In this study, MCAM data showed that samples were distributed into low/high methylation groups (bimodal distribution), suggesting the existence of CIMP in meningiomas (Figure 1C). Indeed, among nine tumors with >350 methylated genes (i.e. hypermethylated tumors), majority of the tumors (eight tumors) were classified into cluster 3, which correlated well with the tumor aggressiveness. In addition, we provided here five potent markers, which effectively predict CIMP in meningiomas. Additionally, as an important finding in the present study, there were early alterations and stabilities of methylation status in malignant transformation cases (Figure 3D). This suggests two theories: (i) biological alterations including DNA methylation might be acquired before histological changes or (ii) aberrant methylation might be a predictor of malignant transformation as well as recurrence.

The five genes chosen in the present study are potential epigenetic biomarkers, but their association with several hematopoietic or solid tumors is interesting as demonstrated in previous studies. For example, the homeobox (*HOX*) family is a target for silencing by DNA methylation and polycomb complexes (29–31). The comethylation of *HOX* genes, including *HOXA6*, leads to the downregulation of protein expression and dysfunction as tumor suppression genes and is frequently identified in adult chronic lymphocytic leukemia and childhood acute lymphocytic leukemia (32). *HOXA9* has been reported to be a methylation marker of ovarian tumors (33) and squamous cell lung carcinomas (34). Additionally, a CIMP-like accumulation of methylated genes, including *HOXA9*, is detected in aggressive mantle cell lymphoma (35). The *HOX* family tends to show comethylation even between different *HOX* clusters (32); however, only *HOXA* cluster genes in 7p15.2, such as *HOXA5*, *HOXA6*, *HOXA9* and *HOXA11*, were frequently methylated, whereas other *HOX* clusters (*HOXB*, *HOXC* and *HOXD*) showed low methylation among all samples in our study (data not shown). This suggests the correlation between concordant methylation in the *HOXA* cluster and tumorigenesis or character formation in meningiomas. On the other hand, *PENK* methylation is reported in pancreatic cancers (36), bladder cancers (37) and pulmonary adenocarcinomas (38). *PENK* tends to be detected as one of a subset of aberrant methylated genes (37,38), similar to our present results. *UPK3A* alterations are mainly reported in urothelia and neoplasms, but recently an aberrant methylation of *UPK3A* has also been shown to be associated with the distant metastasis in colorectal cancers (39). *IGF2BP1* (*IMP-1/CRDBP*) is an RNA-binding protein that regulates messenger RNA localization, stability and translocation. The *IGF2BP1* protein is actively expressed during embryogenesis and is also considered to play a role in tumorigenesis by stabilizing messenger RNAs of the *c-myc* oncogene and *IGF2* in certain cancers (40). On the other hand, it is reported that the *IGF2BP1* knockdown

by RNA interference increases the proliferation in leukemia K562 cells (41), and silencing by promoter methylation accelerates the growth of tumor cells and migration of human breast cancer cells (42). The biological implications of *IGF2BP1* methylation and functioning mechanisms in tumor cells remain uncertain, and they might differ among tumors of different origins.

In conclusion, this is the first study indicating the presence of subgroups with aberrant accumulation of promoter methylation in WHO grade I and II meningiomas. These alterations correlate with high frequency of recurrence and may occur in the initial stage of histological changes such as malignant transformation. Our findings highlight the possibility of speculating individuals with malignant characteristics from low-grade meningiomas by quantifying methylation of certain genes.

Supplementary material

Supplementary Tables 1–4 and Figures 1–3 can be found at http://carcin.oxfordjournals.org/.

Conflict of Interest Statement: None declared.

Funding

PRESTO of JST (to Y.K.), Grant-in-Aid for Scientific Research from the Japan Society for the Promotion of Science (to Y.K., A.N.).

References

1. Maier,H. *et al*. (1992) Classic, atypical, and anaplastic meningioma: three histopathological subtypes of clinical relevance. *J. Neurosurg.*, **77**, 616–623.
2. Perry,A. *et al*. (1997) Meningioma grading: an analysis of histologic parameters. *Am. J. Surg. Pathol.*, **21**, 1455–1465.
3. Aghi,M.K. *et al*. (2009) Long-term recurrence rates of atypical meningiomas after gross total resection with or without postoperative adjuvant radiation. *Neurosurgery*, **64**, 56–60; discussion 60.
4. Perry,A. *et al*. (1999) ''Malignancy'' in meningiomas: a clinicopathologic study of 116 patients, with grading implications. *Cancer*, **85**, 2046–2056.
5. Willis,J. *et al*. (2005) The accuracy of meningioma grading: a 10-year retrospective audit. *Neuropathol. Appl. Neurobiol.*, **31**, 141–149.
6. Al-Mefty,O. *et al*. (2004) Malignant progression in meningioma: documentation of a series and analysis of cytogenetic findings. *J. Neurosurg.*, **101**, 210–218.
7. Hancq,S. *et al*. (2004) S100A5: a marker of recurrence in WHO grade I meningiomas. *Neuropathol. Appl. Neurobiol.*, **30**, 178–187.
8. Lusis,E.A. *et al*. (2005) Integrative genomic analysis identifies NDRG2 as a candidate tumor suppressor gene frequently inactivated in clinically aggressive meningioma. *Cancer Res.*, **65**, 7121–7126.
9. Surace,E.I. *et al*. (2004) Loss of tumor suppressor in lung cancer-1 (TSLC1) expression in meningioma correlates with increased malignancy grade and reduced patient survival. *J. Neuropathol. Exp. Neurol.*, **63**, 1015–1027.
10. Nunes,F. *et al*. (2005) Inactivation patterns of NF2 and DAL-1/4.1B (EPB41L3) in sporadic meningioma. *Cancer Genet. Cytogenet.*, **162**, 135–139.
11. Jones,P.A. *et al*. (2007) The epigenomics of cancer. *Cell*, **128**, 683–692.
12. Barski,D. *et al*. (2010) Hypermethylation and transcriptional downregulation of the TIMP3 gene is associated with allelic loss on 22q12.3 and malignancy in meningiomas. *Brain Pathol.*, **20**, 623–631.
13. McShane,L.M. *et al*. (2005) REporting recommendations for tumour MARKer prognostic studies (REMARK). *Br. J. Cancer*, **93**, 387–391.
14. Toyota,M. *et al*. (1999) Identification of differentially methylated sequences in colorectal cancer by methylated CpG island amplification. *Cancer Res.*, **59**, 2307–2312.
15. Colella,S. *et al*. (2003) Sensitive and quantitative universal Pyrosequencing methylation analysis of CpG sites. *Biotechniques*, **35**, 146–150.
16. Gao,W. *et al*. (2008) Variable DNA methylation patterns associated with progression of disease in hepatocellular carcinomas. *Carcinogenesis*, **29**, 1901–1910.
17. Goto,Y. *et al*. (2009) Epigenetic profiles distinguish malignant pleural mesothelioma from lung adenocarcinoma. *Cancer Res.*, **69**, 9073–9082.
18. Okamoto,Y. *et al*. (2011) Aberrant DNA methylation associated with aggressiveness of gastrointestinal stromal tumour. *Gut*. Epub ahead of print. doi:10.1136/gut.2011.241034.
19. Verhaak,R.G. *et al*. (2010) Integrated genomic analysis identifies clinically relevant subtypes of glioblastoma characterized by abnormalities in PDGFRA, IDH1, EGFR, and NF1. *Cancer Cell*, **17**, 98–110.
20. Monti,S. *et al*. (2003) Consensus clustering: a resampling-based method for class discovery and visualization of gene expression microarray data. *Mach. Learn.*, **52**, 91–118.
21. Shen,L. *et al*. (2005) MGMT promoter methylation and field defect in sporadic colorectal cancer. *J. Natl. Cancer Inst.*, **97**, 1330–1338.
22. Shen,L. *et al*. (2007) Integrated genetic and epigenetic analysis identifies three different subclasses of colon cancer. *Proc. Natl Acad. Sci. USA*, **104**, 18654–18659.
23. Zhang,X. *et al*. (2010) Maternally expressed gene 3, an imprinted noncoding RNA gene, is associated with meningioma pathogenesis and progression. *Cancer Res.*, **70**, 2350–2358.
24. Nakane,Y. *et al*. (2007) Malignant transformation-related genes in meningiomas: allelic loss on 1p36 and methylation status of p73 and RASSF1A. *J. Neurosurg.*, **107**, 398–404.
25. Kandenwein,J.A. *et al*. (2011) uPA/PAI-1 expression and uPA promoter methylation in meningiomas. *J. Neurooncol.*, **103**, 533–539.
26. Toyota,M. *et al*. (1999) CpG island methylator phenotype in colorectal cancer. *Proc. Natl Acad. Sci. USA*, **96**, 8681–8686.
27. Toyota,M. *et al*. (1999) Aberrant methylation in gastric cancer associated with the CpG island methylator phenotype. *Cancer Res.*, **59**, 5438–5442.
28. Noushmehr,H. *et al*. (2010) Identification of a CpG island methylator phenotype that defines a distinct subgroup of glioma. *Cancer Cell*, **17**, 510–522.
29. Morgan,R. (2006) Hox genes: a continuation of embryonic patterning? *Trends Genet.*, **22**, 67–69.
30. Lee,T.I. *et al*. (2006) Control of developmental regulators by Polycomb in human embryonic stem cells. *Cell*, **125**, 301–313.
31. Soshnikova,N. *et al*. (2008) Epigenetic regulation of Hox gene activation: the waltz of methyls. *Bioessays*, **30**, 199–202.
32. Strathdee,G. *et al*. (2007) Inactivation of HOXA genes by hypermethylation in myeloid and lymphoid malignancy is frequent and associated with poor prognosis. *Clin. Cancer Res.*, **13**, 5048–5055.
33. Wu,Q. *et al*. (2007) DNA methylation profiling of ovarian carcinomas and their *in vitro* models identifies HOXA9, HOXB5, SCGB3A1, and CRABP1 as novel targets. *Mol. Cancer*, **6**, 45.
34. Rauch,T. *et al*. (2007) Homeobox gene methylation in lung cancer studied by genome-wide analysis with a microarray-based methylated CpG island recovery assay. *Proc. Natl Acad. Sci. USA*, **104**, 5527–5532.
35. Enjuanes,A. *et al*. (2011) Identification of methylated genes associated with aggressive clinicopathological features in mantle cell lymphoma. *PLoS One*, **6**, e19736.
36. Ueki,T. *et al*. (2001) Identification and characterization of differentially methylated CpG islands in pancreatic carcinoma. *Cancer Res.*, **61**, 8540–8546.
37. Chung,W. *et al*. (2011) Detection of bladder cancer using novel DNA methylation biomarkers in urine sediments. *Cancer Epidemiol. Biomarkers Prev.*, **20**, 1483–1491.
38. Chung,J.H. *et al*. (2011) DNA methylation profile during multistage progression of pulmonary adenocarcinomas. *Virchows Arch.*, **459**, 201–211.
39. Ju,H.X. *et al*. (2011) Distinct profiles of epigenetic evolution between colorectal cancers with and without metastasis. *Am. J. Pathol.*, **178**, 1835–1846.
40. Ioannidis,P. *et al*. (2005) CRD-BP/IMP1 expression characterizes cord blood CD34+ stem cells and affects c-myc and IGF-II expression in MCF-7 cancer cells. *J. Biol. Chem.*, **280**, 20086–20093.
41. Liao,B. *et al*. (2004) Targeted knockdown of the RNA-binding protein CRD-BP promotes cell proliferation via an insulin-like growth factor II-dependent pathway in human K562 leukemia cells. *J. Biol. Chem.*, **279**, 48716–48724.
42. Gu,W. *et al*. (2009) Blocking beta-catenin binding to the ZBP1 promoter represses ZBP1 expression, leading to increased proliferation and migration of metastatic breast-cancer cells. *J. Cell Sci.*, **122**, 1895–1905.

Received July 3, 2011; revised November 2, 2011; accepted November 13, 2011